DOI: 10.17580/cisisr.2020.01.12

UNDERSTANDING THE STRUCTURE AND PROPERTIES OF THE HEAT AFFECTED ZONE IN WELDS AND MODEL SPECIMENS OF HIGH-STRENGTH LOW-ALLOY STEELS AFTER SIMULATED HEAT CYCLES

E. I. Pryakhin[1], D. M. Sharapova[1]

[1] *St. Petersburg Mining University (St. Petersburg, Russia)*

E-mail: e.p.mazernbc@yandex.ru

AUTHOR'S INFO

E. I. Pryakhin, Dr. Eng., Prof., Head of Dept. of Material Science,
D. M. Sharapova, Cand. Eng., Assistant

Key words:

low-alloy high-strength steel, electric arc welding, reheating, heat affected zone, microstructure, dilatometric study, impact energy, heat input.

ABSTRACT

Localized heat applied during welding or rebuilding of parts can lead to a noticeable structural evolution in the heat affected zone of the high-strength low-alloy K65 steel. A comprehensive study that was carried out on model and full-scale specimens and looked at the structure and properties of steel in the heat affected zone after single and double heat cycles proved the above trend. Through metallographic and X-ray microstructural analysis, it was found how and in what conditions a brittle phase forms at coarse grain boundaries, the amount of which and the distribution around the grain is in direct relationship with the number of heat cycles and the heat input of the welding procedure. It was established that during the initial heat cycle the new phase around the grains tends to grow as the cooling rate goes down, which is consistent with the reduced toughness of steel in the heat affected zone during high heat input welding. When the HAZ is reheated, the undesirable structural changes become even more pronounced. The results of the study show that the steel in view does not provide enough workability and that a specification is required to limit the amount of heat input introduced during the initial and further heat cycles in welding.

Introduction

Today's manufacturing industry vastly relies on various sources of heat that produce certain effects on the material. Heat can be applied during manufacturing or rebuilding of parts in order to eliminate defects and restore parts and their performance. Such effects include a structural evolution of metal. Short-term high-temperature impacts alter the physico-mechanical properties of the material (leading to localized degradation) affecting the parts' performance and repairability. The problem of evolving structure and properties of steels for weld joints has recently been in the focus of attention [1–6].

Structural evolution and localized degradation of material subjected to short-term heat impacts are governed by heat propagation through the part, which is dictated by the part design, heat entry point, the thermophysical properties of the material, as well as the type, activity and power of the heat source. The temperature field determines the structure and properties of the weld material in the heat affected zone (HAZ) [4], which are governed by the chemical composition of the material of the welded parts.

Welding technology is widely used in manufacturing and is universal in building and rebuilding of parts. Repeated heat impacts occur in double and multi pass welding and in almost all part rebuilding procedures involving arc welding. They lead to a nonuniform structure with different mechanical properties formed in both the weld seam and the HAZ. Such nonuniform structure can easily be identified on macrostions.

In recent years, researchers have given a great deal of attention to the problem of ensuring strength in the HAZ when welding high-strength low-alloy steels [7–8]. However, certain problems related to the repairability of high-strength low-alloy steel parts by welding still await thorough investigation [9–10]. A new type of structural evolution has been established in the HAZ when studying K65 steel weld joints produced by double pass high heat input welding. Specific structural changes have been identified through metallographic study. They can be observed at coarse grain boundaries in the overheated area of the first pass HAZ after the sond heat impact occurring during the sond weld pass. At the same time, a series of Charpy impact tests was carried out with weld joints done on standard pipes by different manufacturers. The specimens were tested at minus 40 °C with the notch done in the specified area of the HAZ. The energy as low as 37 J was registered as a result, which does not conform with the specification applicable to this steel grade ($KV_{min} = 47$ J). At the same time, no such structural changes were observed in the overheated area after single pass welding, and no impact energy below the allowable limit was registered in the course of the Charpy tests.

In view of the above, it was crucial to investigate and understand the mechanism behind and the kinetics of structural evolution and mechanical degradation in the HAZ of high-strength low-alloy steels subjected to multiple pass welding.

Aim of Research

This research aims to establish a relationship between the bending impact test results and the observed structure formed in the HAZ in K65 steel as a result of double pass welding associated with a double heat cycle.

Table 1. **Chemical Composition of Semiproducts**

K65 steel	C	Si	Mn	P	S	Cr	Ni	Cu	Mo	Al	N	Ti	Nb	V	C_{eqv}	Fracture strength R_{sm}
Semiproduct 1	0.06	0.20	1.78	0.005	0.002	0.09	0.24	0.05	0.22	0.03	0.005	0.020	0.06	0.020	0.44	0.18
Semiproduct 2	0.06	0.24	1.82	0.005	0.002	0.03	0.27	0.27	0.20	0.03	0.007	0.018	0.05	0.025	0.45	0.19

Table 2. **Mechanical Properties of Semiproducts**

Semiproduct	Actual Values						Specification (≥)			
	Yield Strength σ_T, MPa	Ultimate Tensile Strength σ_B, MPa	δ, %	KV^{-40}, J/cm^2			Yield Strength σ_T, MPa	Ultimate Tensile Strength σ_B, MPa	δ, %	KV^{-40}, J/cm^2
1	593	664	20	273	250	248	555	640	18	200
2	660	723	21	280	283	284	555	640	18	200
Impact energy of weld joint steel per Specification									KV^{-40}, J	
Average of 3 tests									65	
Minimum value									47	

Materials and Methods of Research

For the purpose of this research, K65 pipe steel was used in the experiments. Two types of semiproducts were used (**Table 1 and 2**).

As the use of destructive techniques to study the effect of heat impact on the structure and properties of material in the HAZ can be costly, modelling of heat impacts becomes of great relevance.

Considering the relevance of the above circumstances, the main experimental study for this research was based on the results of mathematical modelling of heat processes when heat sources produced localized impacts on the material (like in welding) [11–14]. The following model was used for the purpose of this study, which was developed by the authors together with V. N. Startsev [15]:

$$\rho C_p V dT/dx = \text{div}\,(\lambda\,\text{grad}\,T + S), \quad (1)$$

where ρ – density; C_p – heat capacity; V – heat source travel rate; T – temperature; x – heat source travel direction (coordinate); λ – heat conductivity; S – spatial heat sources.

Numerical solution for this equation was found with the help of the Flex-EDF program.

This model can successfully be used to calculate heat cycle parameters in welding. It gives an adequate description of the thermal environment in arc gouging and can be used for heat calculations in surfacing.

The structural evolution of steel under thermal impacts in process was studied through physical modelling of real thermal processes in the HAZ. By means of mathematical modelling, typical thermal cycles were identified, which were implemented on the dilatometer DIL 805 when simulating the heat impact in the HAZ of the studied steels.

A single heat impact on metal in the HAZ was simulated on model specimens, which were heated to maximum temperatures T_{max}: 1,350; 1,100; 900, 800, 750, 700 °C. This was correlated with the temperature fields in different HAZ areas. The specimens were cooled down at the rates ω within the range from 1 to 100 °C/s. Exact cooling rates were established following a comparison of the resultant structures with the structures obtained after a double heat impact.

Table 3. **Multiarc Welding Modes**

Parameters	Electrode No.				
	1	2	3	4	5
Welding current, A	1150	900	800	750	650
Voltage, V	32	34	37	39	40
Welding speed, m/min	2				
Stick-out distance, mm	28				
Heat input, kJ/mm	4.6				

Based on the calculated cooling rates in the HAZ and considering the actual heat cycles in double pass welding, the following cooling rate was established for model specimens for the first heat cycle: $\omega_1 = 50$ °C/s ($T_{max_1} = 1{,}350$ °C). Additionally, structures were studied that formed at the cooling rate of $\omega_1 = 20$ °C/s. Such cooling rate is possible if the temperatures exceed Ac_3 in the case of high heat inputs (5–6 kJ/mm). At the T_{max_1} temperatures of 1,000 to 700 °C, the actual cooling rates are lower. When the maximum temperatures drop to 800–700 °C, the observed cooling rates can drop twice. That is why the T_{max_2} temperatures of 950 to 700 °C with the step of 50 °C were selected for simulation of the sond pass, and the cooling rates ω_1 were established at 1 and 5 °C/s.

It should be noted that for the weldability index C_{eqv} and the fracture strength R_{sm}, the studied steel could be welded without being preheated. If preheat was required, it would need to be accounted for in heat cycle modelling.

Table 3 shows the welding modes applied to the steel in view.

This research also involved an X-ray microstructural analysis, a metallographic study of stions, as well as standard mechanical and hardness tests.

Obtained Results and Discussion

With the help of dilatometric curves, the start (T_s) and finish (T_f) temperatures were determined during

simulation of phase transformations occurring when austenite was cooling down in the HAZ of the studied steels [8]. It is demonstrated that irrespective of the heat input and provided $\omega_{8/5}$ = = const, austenite becomes more stable as the maximum heating temperature T_{max} goes down and the steel strength decreases. It was established that, within the temperature range of 800 to 500 °C, as the cooling rate $\omega_{8/5}$ rises, the temperature median T_{md} of the austenitic transformation range goes down linearly, which is determined by the dependencies (2a) and (2b). The steel with higher strength has a lower austenitic stability.

$$T_{md_1} = 570 - 1.6\omega_{8/5}; \quad (2a)$$

$$T_{md_2} = 530 - 1.6\omega_{8/5}; \quad (2b)$$

where the median $T_{md} = 0.5(T_s - T_f)$ defines the median values of the temperature range associated with austenitic transformation.

The dependencies (2*a*) and (2*b*) are true within the following range: 1,350 °C ≥ T_{max} ≥ ≥ 900 °C.

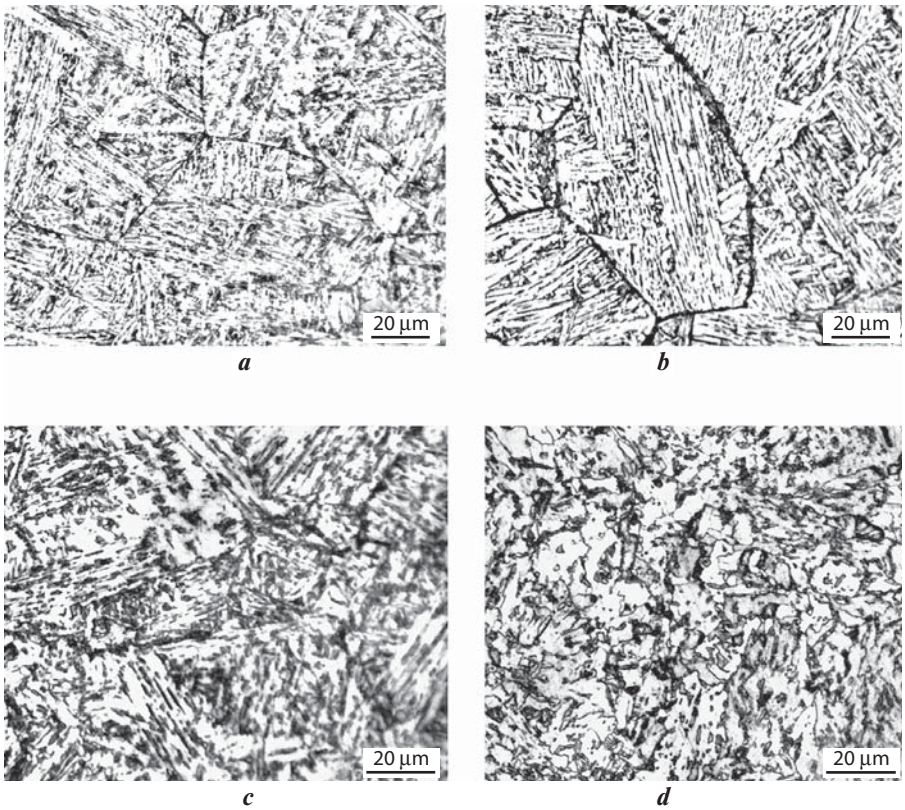

Fig. 1. Structural changes in the simulated K65 steel specimens after a double heat cycle at 1,350 °C — 20 °C/s + T_{max_2} — 5 °C/s as a function of T_{max_2}: *a* — 1,350 °C – 20 °C/s + 700 °C – 5 °C/s; *b* – 1,350 °C – 20 °C/s + + 750 °C – 5 °C/s; *c* —1,350 °C – 20 °C/s + 800 °C – 5 °C/s; *d* — 1,350 °C – 20 °C/s + 900 °C – 5 °C/s

The results of simulated double heat cycles show that the sond heat cycle with the following parameters: 850 °C < T_{max_2} < 950 °C and $\omega_2 \geq 10$ °C/s, leads to greater changes in the steel structure in the HAZ resultant from the first heat cycle. A high degree of structural refinement was observed at the heating temperature of T_{max_2} = 950 °C.

Separate areas with a new phase forming can be seen at coarse grain boundaries when the area is heated to T_{max_2} = = 700 °C (**Fig. 1, *a***). As the temperature rises to T_{max_2} = = 750 °C, these areas get bigger merging together around the grains (**Fig. 1, *b***). However, if the maximum temperature reaches $T_{max_2} > A_{c1}$, the new phase stops growing. And if the maximum temperature continues rising, the generation of the new phase becomes less active. At T_{max_2} = = 800 °C the areas with the new phase at grain boundaries look like chains (**Fig. 1, *c***), while at T_{max_2} = 950 °C they disappear altogether (**Fig. 1, *d***).

How and how much of the new phase gets generated is dictated by the cooling rates in the first and sond heat cycles.

In a double heat cycle applied to model specimens, two options were simulated on the dilatometer for the first heat cycle while the sond heat cycle was constant: Option 1 – 1,350 °C – 50 °C/s + 750 °C – 5 °C/s; Option 2 – 1,350 °C – 20 °C/s + 750 °C – 5 °C/s. It was found that the generation of the new phase around the grains becomes more intense when the cooling rate in the first heat cycle ω_1 is lower. But we know that a decreasing cooling rate of metal in the HAZ is associated with a rising heat input. So, one of the key factors leading to a lower toughness of metal in the HAZ can be linked to high heat inputs, which are usually applied for better welding performance.

In dilatometric simulation of the double heat cycle, different modes of the sond heat cycle were also tested while the first heat cycle remained constant: Option 1 — 1,350 °C — 20 °C/s + 750 °C — 1 °C/s; Option 2 — 1,350 °C — 20 °C/s + 750 °C — 5 °C/s. It was found that the generation of the new phase at grain boundaries becomes more intense when the cooling rate in the sond heat cycle ω_2 is higher. However, since the new phase areas start growing in the temperature range of 700–800 °C as the cooling rate rises in the sond heat cycle, the assumption that the generation of the new phase is due to carbides formed in the HAZ structure fails to prove true.

The main conditions for a new phase to form around the grains when the HAZ steel is heated include as follows:

- coarse grains got formed during the first heat cycle (when the temperature significantly exceeded A_{c3}) over a short time frame (within a few sonds);
- the rate of diffusion at grain boundaries is quite high (hundreds of times higher than the rate of diffusion in the grains).

Because of this, the areas adjacent to the grain boundaries get enriched with carbon and alloying elements. But because the process goes so fast, there is not enough time for the chemical composition to become uniform across the grain. Such chemical non-uniformity is not a new phenomenon. For example, it is demonstrated in paper [16] that looked at the HAZ in the steel grade 10GN2MFA. The results presented in this paper suggest that a similar enrichment with alloying elements takes place at grain boundaries in the overheated area in the HAZ. But we know that a higher concentration of alloying elements in steel leads to decreased critical points A_{c1} and A_{c3}.

In the intercritical range — i.e. 800–900 °C — austenite starts to form not only at grain boundaries but also in the grains. As the austenite that formed at grain boundaries gets less enriched with carbon or alloying elements (as compared with the heat reaching 750 °C), it becomes less stable during cooling. If one can still observe some martensite/bainite around separate grains at the cooling rate of 5 °C/s following heating to 800 °C, when the cooling rate gets to 1 °C/s, bainitic ferrite precipitates during early $\gamma \rightarrow \alpha$ transformation (see Fig. 1).

The heating temperature reaching 900 °C (above A_{c3}) triggers an overall structural recrystallization: the boundaries of the initial coarse grains disappear, but the chemical non-uniformity is still present, and separate martensitic/bainitic areas can be seen where grain boundaries used to be.

So, a relationship was found between the simulated heat modes and the observed structures during the first heat cycle having the following parameters: $T_{\max_1} \times \omega_1 = 1{,}350\ ^\circ\text{C} \times 50^\circ\text{C/s}$, and the sond heat cycle involving the following maximum temperatures: $T_{\max_2}$ = 700–800 °C, and cooling rates: 1–5 °C/s.

During the sond heat cycle, due to non-uniform alloying, areas get formed at grain boundaries in which the critical point A_{c1} is lower (700–750 °C) than in the grain body (780 °C). It is in this region where the sond phase (supposedly, a mix of martensite and bainite) starts to form. This is the very structure that is observed in the HAZ of actual welds during transformation of non-homogeneous austenite at grain boundaries.

Consequently, enrichment of steel with alloying elements can lead to decreased critical points at separate locations (close to the boundaries). It is in these areas that austenite enriched with alloying elements precipitates at grain boundaries during the sond heat cycle when the steel is heated to the temperatures below A_{c1}. During the following cooling cycle austenite undergoes transformation. One can see that in the microstructure as dark etching areas of the new phase located around coarser grains. The new phase includes high-carbon martensite or a mix of martensite and bainite. This effect becomes more pronounced as a result of the sond heat cycle in the temperature range ($A_{c1} - 30\ ^\circ\text{C} < T_{\max_2} < A_{c1}$). Further heat cycles (no. 3, 4 and so on) lead to a greater chemical non-uniformity at grain boundaries. Consequently, at high cooling rates the brittle martensite/bainite constituent becomes larger.

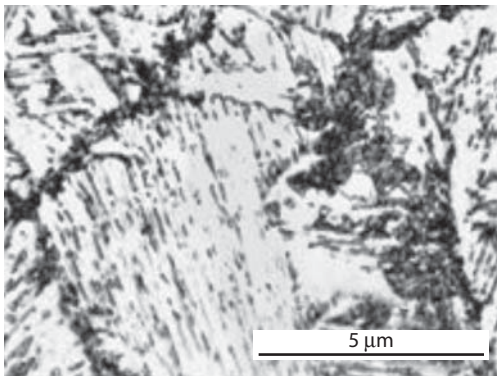

Fig. 2. Microstructure of a K65 steel model specimen after the initial heat cycle at (1,350 °C — 50 °C/s) and the following five consutive heat cycles at (750 °C — 5 °C/s)

An additional experiment was conducted to further study the new structure. After the first heating on the dilatometer at 1,350 °C — 50 °C/s, the model specimens were subjected to multiple heat cycles based on the following parameters: 750 °C — 5 °C/s. It was found that, after the following five consutive heat cycles (**Fig. 2**), the microstructure of the studied steel consists of grains with fine needle-shaped crystals at their boundaries.

X-ray microstructural analysis of the model specimens after the simulated heat cycles confirmed the supposition that the dark etching areas of the new phase at grain boundaries have a martensitic/bainitic structure enriched with alloying elements. The analysis results indicate a noticeable redistribution of the main alloying elements (such as Mn, Ni, Mo, V). Thus, their concentration tends to rise in the new phase areas at grain boundaries, while in the regions adjacent to the grain boundaries their concentration is lower (**Fig. 3, Table 4**).

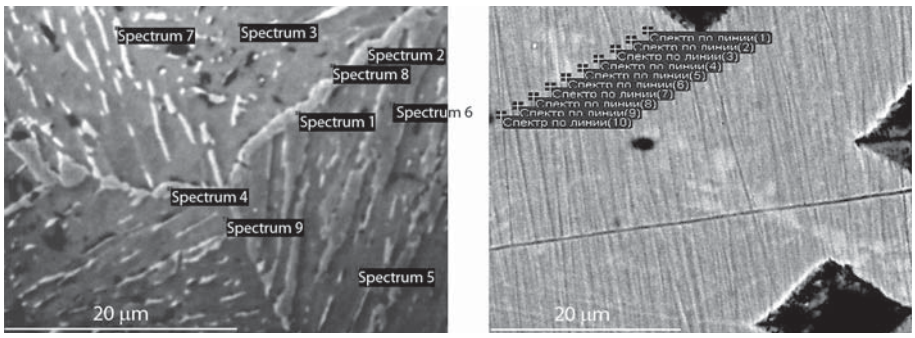

Fig. 3. Electronic image of the model specimens' metal during X-ray microstructural analysis

Table 4. **X-Ray Microstructural Analysis Data: Concentrations of Key Alloying Elements, %**

Studied Area	Mn	Ni	Mo	V
Grain boundary	2.05	0.35	0.26	0.028
Near the grain boundary	1.51	0.26	0.19	0.020
Average concentration in steel	1.78	0.24	0.22	0.020

In addition to the metallographic study, a series of microhardness tests was carried out in which microhardness was measured near the grain boundaries, in the grain core and at the boundaries. The tests showed that the microhardness of the new phase at grain boundaries is 415 ± 15HV, which is ≈15% higher than that near the grain boundaries (365 ± 5HV) and ≈20% higher than the microhardness in the grain core (345 ± 5HV). These figures support the conclusion that the new phase at grain boundaries is highly brittle, and this explains the reduced toughness of steel in the HAZ. This is also indicated by the results of microhardness tests conducted on specimens that were heated to different modes during dilatometric simulation. The microhardness of the studied structures would not exceed 370 ± 5HV in any of the test areas.

To confirm the data obtained from testing the model specimens, additional tests were carried out that focused on the material cut out from the HAZ of welds on real parts. The results showed a good consistency proving a direct link between the martensitic or martensitic/bainitic structures that occur at the boundaries of coarser grains in the HAZ following repeated heat cycles and the lower toughness of steel in the HAZ.

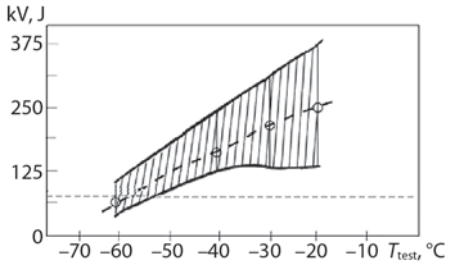

Fig. 4. Results of bending impact tests for K65 steel welds

A separate study that examined the mechanical properties of welds in the HAZ showed that certain areas of the HAZ have low toughness. At –60 °C, the average impact energy on Charpy specimens with a notch made in the HAZ close to the weld line in the area that was reheated in the sond weld pass does not exceed 60 J (**Fig. 4**), and hardness is within 330–360 HV. Tests conducted with Charpy specimens with a notch being 2 mm away from the weld zone indicate a significantly higher toughness (on some specimens the impact energy reached 200 J), while hardness was 220–230 HV. This is consistent with the structural changes that took place in the model specimens after the heat cycles simulated on the dilatometer. These results indicate that steel may have toughness below the specified level when conducting bending impact tests for material from the HAZ of standard parts.

The study showed that the lower toughness of the material in the HAZ resultant from double or multiple weld heat cycles is linked to the structural evolution of metal under strong heat input conditions. On the one hand, this can explain the regularities of material degradation during localized short-term heat impacts. On the other hand, this relationship can be of great practical relevance for machine shops that manufacture or repair parts made of low-alloy steels.

The need to account for the repairability of steel is confirmed by the results of a study that looked at a number of steel specimens after simulation. It is also confirmed by the data on standard parts and test samples. **Fig. 5, *a*** shows the steel structure of a real part after a single heat cycle. For the sake of comparison, the same figure shows the boundaries of a coarse grain that formed in the structure of model specimens after a high-temperature single heat cycle (**Fig. 5, *b***) and simulated multiple heat cycles (**Fig. 5, *c***).

Verification of the model specimens study results, as well as analysis of test data obtained from the test samples and real machine parts made of the studied steel prove that there is a relationship between the structural evolution of metal in the HAZ and the low impact energy associated with the high energy input occurring during a double heat cycle. Hence, the conclusion to be drawn

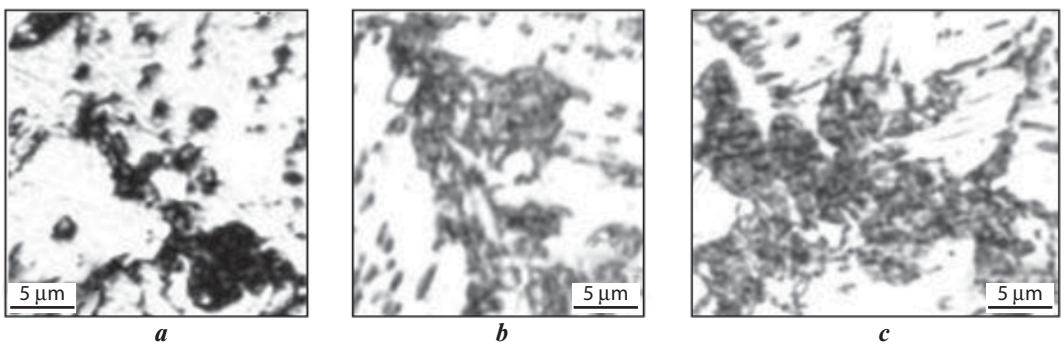

a ***b*** ***c***

Fig. 5. Microstructure of K65 steel — grain boundaries:
a — stion of a coarse grain in the HAZ of a real part after a single heat cycle; *b* — simulation specimen after a single heat cycle at: 1,350 °C — 50 °C/s; *c* — simulation specimen after a double heat cycle at: 1,350 °C — 50 °C/s + 750 °C — 5 °C/s; *d* — simulation specimen after multiple heat cycles at: 1,350 °C — 50 °C/s and five consutive heat cycles at: 750 °C — 5 °C/s

is that appropriate limits with regard to the heat input should be introduced in welding.

Conclusion

A comprehensive study that looked at the structure and mechanical properties of welds in standard machine parts, test samples and model specimens made of high-strength low-alloy K65 pipe steel indicated that repeated short-term heat impacts occurring in the heat affected zone are associated with degradation of the material performance, which is due to the formation of martensitic/bainitic structures enriched with carbon and alloying elements, which precipitate at coarse grain boundaries following high-temperature double or multiple heat cycles. It was established that the steel in view does not provide enough workability. That is why a specification is required to limit the amount of heat input introduced during the initial and further heat cycles in multipass welding.

REFERENCES

1. Shchipachev A. M., Gorbachev S. V. Effect of post weld heat treatment on the rate of general corrosion and the microstructure of weld joints on Steel 20 and Steel 30KhGSA. *Zapiski Gornogo instituta*. 2018. Vol. 231. pp. 307–311.
2. Kirian V. I., Mikhoduy L. I. Problems related to the use of new extra-high and high strength steels in welded structures. *Avtomaticheskaya svarka*. 2002. No. 3. pp. 10–17.
3. Golosienko S. A., Ilyin A. V., Lavrentiev A. A., Mikhailov M. S., Motovilina G. D., Petrov S. N., Sadkin K. E. Brittle fracture resistance of high-strength medium-alloy steel and how it is related to the structural state parameters. *Voprosy materialovedeniya*. 2019. No. 3 (99). pp. 128–147.
4. Velichko A. A., Bortsov A. N., Shabalov I. P., Frantov I .I., Utkin I. Yu. Relationship between heat processes and the weld morphology and innovative welding techniques applicable to thick-walled electric-welded pipes. *Metallurg*. 2014. No. 3. pp. 72–77.
5. Thiessen R. G., Paul G., Sebald R. Innovative high-strength steels with enhanced mechanical parameters. *Chernye Metally*. 2019. No. 8. pp. 51–55.
6. Oryshchenko A. S., Pimenov A.V., Shekin S. I., Sharapov M. G. Understanding the effect of nonmetallic inclusions on the weld toughness of cold-resistant steels at low temperatures. *Svarochnoe proizvodstvo*. 2012. No. 8. pp. 6–11.
7. Hamada M. Control of strength and toughness at the heat affected zone. *Welding International*. 2003. No. 17(4). pp. 265–270.
8. Shi Y., Han Z. Effect of weld thermal cycle on microstructure and fracture toughness of simulated heat-affected zone for a 800 MPa grade high strength low alloy steel. *Journal of Materials Processing Technology*. 2008. Vol. 207. pp. 30–39.
9. Hillenbrand H.-G., Gras M., Kalwa C. Development and production of high strength pipeline steels. *Niobium Science and Technology: Proceedings of the International Symposium on Niobium*. Orlando, Florida. 2001, Dec. 2–5.
10. Meimeth S., Grimpe F., Meuser H. Development, state of the art and future trends in design and production of heavy plates in X80 steel grades. *Steel Rolling 2006, 9th International & 4th European Conferences*. Paris, France. 2006, June 19–21.
11. Shkatov V. V., Mazur I. P., Knapinski M., Chetverikova T. S. Simulation of dynamic recrystallization and resistance to deformation of carbon and low-alloyed steels during hot forming. *Chernye Metally*. 2018. No. 11. pp. 22–27.
12. Erofeev V. A., Maslennikov A. V. Multipass arc welding procedure and its physico-mathematical model. *Izvestiya Tulskogo gosudarstvennogo universiteta. Seriya: Kompyuternye tekhnologii v soedinenii materialov*. 2005. No. 3. pp. 246–255.
13. Ueda J., Muracawa H., Luo Ju. A. Computational model of phase transformation for welding processes. *Translation of JWRI*. 1995. Vol. 24. No. 1, pp. 95–100.
14. Rao R. V., Kalyankar V.D. Multi-pass turning process parameter optimization using teaching–learning-based optimization algorithm. *Scientia Iranica*. 2013. Vol. 20. Issue 3. pp. 967–974.
15. Makarchuk A. V., Makarchuk N. V., Startsev V. N. Multipass arc welding procedure: Developing a mathematical model. *Vestnik gosudarstvennogo universiteta morskogo i rechnogo flota imeni admirala S.O. Makarova*. 2017. Vol. 9. No. 1. pp. 121–131.
16. Zubchenko A. S., Fedorov A. V., Nechaev Yu. V. Understanding what causes cracking of weld joints on thick-walled pressure vessel under further heat treatment. *Svarka i diagnostika*. 2009. No. 2. pp. 21–25.